Journal of Materials Science and Chemical Engineering, 2016, 4, 35-40
Published Online June 2016 in SciRes. http://www.scirp.org/journal/msce
http://dx.doi.org/10.4236/msce.2016.46005

Kinetics Study on Photocatalytic Degradation of Methyl Orange Catalyzed by Sea Urchin-Like Cu_2O

R. J. Gao[1], T. Ding[1], X. J. Duan[2]

[1]Institutes of Materials Science and Engineering, Ocean University of China, Qingdao, China
[2]Zaozhuang Vocational College of Science and Technology, Zaozhuang, China
Email: dmh206@126.com

Received 22 April 2016; accepted 15 June 2016; published 20 June 2016

Abstract

Sea urchin-like cuprous oxide with hollow glass microsphere as core was prepared using sodium sulfite as the reducing agent and sodium acetate-acetic acid as buffer solution in copper sulfate solution. Methyl orange was selected as degradation target for photocatalytic experiments. The photocatalytic activities were investigated by visible spectro- photometer. Photocatalytic kinetics parameters were studied by the Langmuir-Hinshelwood model and Arrhenius formula. It was observed that the sea urchin-like morphology dramatically improved the photocatalytic activity of cuprous oxide. The photo-degradation belongs to the first-order reaction and the maximum degradation rate could reach 94.37%. The activation energy and pre-exponential factor are 41.18 KJ·mol^{-1} and 1.07 × 10^6, respectively. After seven times recycling, the sample still showed high photo-catalytic efficiency and stability.

Keywords

Cuprous Oxide, Sea Urchin-Like, Photo-Catalyst, Reaction Kinetic, Methyl Orange

1. Introduction

Dye wastewater with the characteristics of complex composition, high color and emissions, high toxicity and poor biodegradability has serious polluted the environment. The common treatment methods of the dye wastewater are flocculation precipitation [1], electrolysis [2], adsorption [3], and biological vectors [4] in industry. One common disadvantage of these methods is that they can transfer the contamination from one phase to another rather than being destructive. Therefore, the invention of a new treatment method without secondary pollution is deemed necessary. In recent years, it has become a focus topic that catalyst is utilized to photodegrade the organic pollutants in wastewater. Cuprous oxide (Cu_2O) has a direct band gap of 2.0 eV which can be excited by visible light, and it has high stability in solar cells [5]. In the past decade, Cu_2O with various morphologies, such as nanosize spheres [6], sea urchin-like [7], porous octahedron [8], nanowires [9] [10], bi-pyramids [11] star-like and flower-like [12], has been synthesized by different techniques. Furthermore, it has

How to cite this paper: Gao, R.J., Ding, T. and Duan, X.J. (2016) Kinetics Study on Photocatalytic Degradation of Methyl Orange Catalyzed by Sea Urchin-Like Cu_2O. *Journal of Materials Science and Chemical Engineering*, **4**, 35-40.
http://dx.doi.org/10.4236/msce.2016.46005

showed an ideal effect on the photocatalytic degradation organic pollutants in water. However, there are rare reports on the photocatalytic kinetics of Cu_2O in previous studies.

In this work, the influence of initial methyl orange (MO) concentration on photo-degradation efficiency was studied. Various kinetics parameters including the reaction rate constants, the activation energy, the pre-exponential factor and the reaction order were obtained and the stability property of the sea urchin-like Cu_2O was also studied.

2. Experimental

Preparation and characterization of the sea urchin-like Cu_2O in detail has been investigated as in [7] and the SEM image of the sea urchin-like Cu_2O shows in **Figure 1**. The sea urchin-like Cu_2O of 0.50 $g{\cdot}L^{-1}$ was added into MO solutions with different initial concentrations according to the corresponding proportion. Then the system was illuminated under a 24 W fluorescent lamp (FSL) after the suspension was stirred in darkness for 40 min to ensure adsorption equilibrium. During the reaction, the beaker filled with the suspension was put into a water-bath to maintain the solution at a constant temperature. The distance between the lamp and the solution surface is 15 cm. The suspension was strongly stirred in order to keep the Cu_2O well suspended in MO solution. During the course of irradiation, 10 mL of the suspension was drawn once from the mixture solution every 5 min and filtrated the Cu_2O. The absorbance of MO aqueous solutions was measured by 7230 G visible spectrophotometer at 464 nm.

3. Results and Discussion

3.1. Effect of Initial MO Concentration on Photodegradation Efficiency

As shown in **Figure 2** the degradation rate of MO first increases and then decreases with the increase of MO concentration from 20 $mg{\cdot}L^{-1}$ to 60 $mg{\cdot}L^{-1}$. And the degradation rate of MO after 25 min reaches 90.9%, 92.23%, 94.37%, 91.48% and 35.35%, respectively.

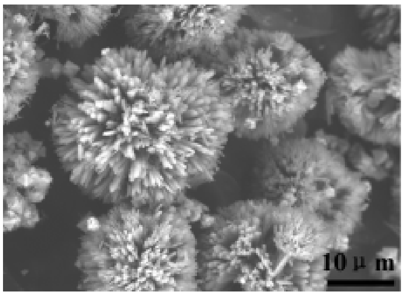

Figure 1. SEM image of the sea urchin-like Cu_2O.

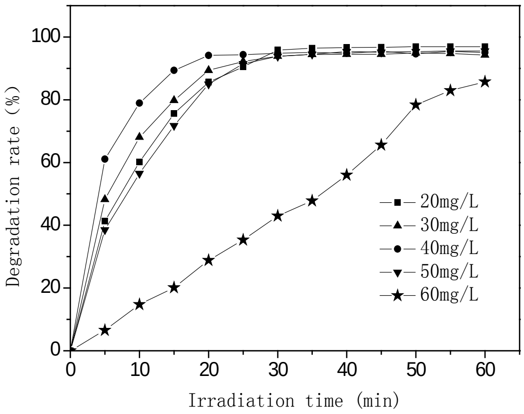

Figure 2. Effect of different initial MO concentration to the degradation rate.

Compared with diffrentCu_2O list in **Table 1**, sea urchin-like Cu_2O showed much higher photocatalytic activity due to the three reasons. (a) Needle-like whiskers increase the surface area that determined by BET method is 3.3961 m^2/g. While the BET surface areas of the octahedral morphology and the truncated octahedral morphology are 0.0308 m^2/g and 0.1819 m^2/g, respectively [13]. (b) The large area exposure of the Cu_2O whiskers, in which visible light can occur numerous times of reflection and diffuse reflection, augments the adsorption ability and utilization rate of visible light. (c) The width size of crystal whiskers of the sea urchin-like Cu_2O is only about 100 nm, so •OH species formed could easily reach the surface of the crystal whiskers to oxidize MO.

3.2. Reaction Order of the Degradation of MO

The degradation of Cu_2O to MO be supposed to first-order kinetics. So, the previous data (before 20 min) taken from **Figure 2** were drawn into plots of $-\ln(C/C_0)$ and irradiation time shown in **Figure 3** The results reveal that the photo-degradation conform the pseudo first-order kinetics really.

3.3. The Activation Energy (Ea) and Pre-Exponential Factor (A) of the Sea Urchin-Like Cu_2O

The temperature can strongly increase the dye degradation, so the activation energy of degredation be studied by the Langmuir-Hinshelwood model [18]. $Cu_2O + hv \rightarrow e^- + h^+$ $OH^- + h^+ \rightarrow \bullet OH$, $\bullet OH + MO \xrightarrow{k_1}$ products. The degradation rate of MO be expressed as: $-\frac{dC_{MO}}{dt} = k_1 C_{\bullet OH} \cdot C_{MO}$. If irradiation time and the amount of Cu_2O are constant, the concentrations of •OH radicals are also constant, $k = k_1 C_{\bullet OH}$, then, $\ln c = -kt + \ln c_0$. In Arrhenius formula: $\ln k = \ln A - \frac{Ea}{RT}$, where, Ea is activation energy and A is pre-exponential factor. In Arrhenius formula: $\ln k = \ln A - \frac{Ea}{RT}$, where, Ea is activation energy and A is pre-exponential factor.

Table 1. The degradation rate of MO in the presence of different Cu_2O.

MO (mg/L^{-1})	Cu_2O ($mg \cdot L^{-1}$)	Time (min)	The degradation rate (%)	References
40	2.00	70	83.49	Tang *et al.* [14]
20	0.20	420	65.5	Huang *et al.* [15]
10	1.00	60	62.5	Zhang *et al.* [16]
20	0.20	30	37	Sun *et al.* [17]
40	0.50	25	94.37	This work

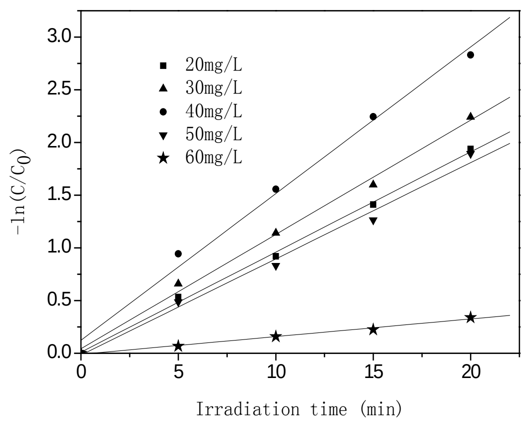

Figure 3. First-order decay curve at different initial MO concentrations.

Figure 4 shows the results of lnk at different temperature, ln*k* are given as: $\ln k = 13.88 - \frac{41183.7}{RT}$.

Ea and A of the degradation are 41.18 KJ·mol^{-1} and 1.07 × 10^6, respectively, with the correlation coefficient of 0.997. Though the raction Ea is little higher than other Cu_2O samples [13]-[15] [19]-[21], the significant increase of A also accelerate the reaction, hence the photo-degradation efficiency of MO is much higher than other Cu_2O samples [13]-[16].

3.4. Photo-Catalytic Efficiency of Seven Times Recycling Use of Catalyst

Stability of Cu_2O was investigated by reuse 7 times shows in **Figure 5** It indicates that the efficiency change from 95.84% to 76.1%. The X-ray patterns of residual Cu_2O after the seventh recycled, as shown in **Figure 6(b)**, is same as before use. So, the sea urchin-like Cu_2O prepared is much stable in the photo-catalysis process under the acidic conditions.

4. Conclusion

The sea urchin-like Cu_2O has highly active to degradation of MO under visible light irradiation. Degradation rate was achieved to 94.37% within 25 min. The photo degradation of MO follows the Langmuir-Hinshelwood model and belonging to the first-order reaction. The activation energy and pre-exponential factor are 41.18 KJ·mol^{-1} and 1.07 × 10^6, respectively. After seven times recycling, the Cu_2O still showed higher photo-catalytic

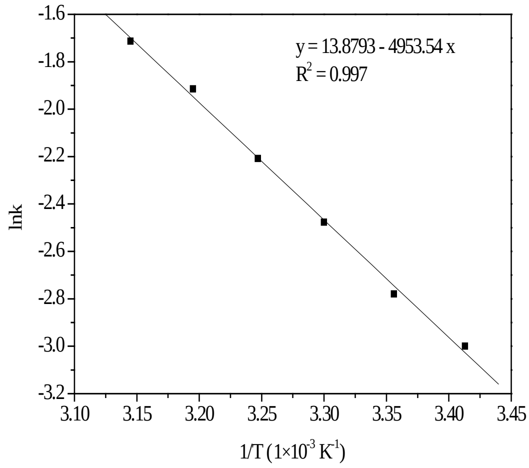

Figure 4. Dependence of the first-order kinetics constant and temperature.

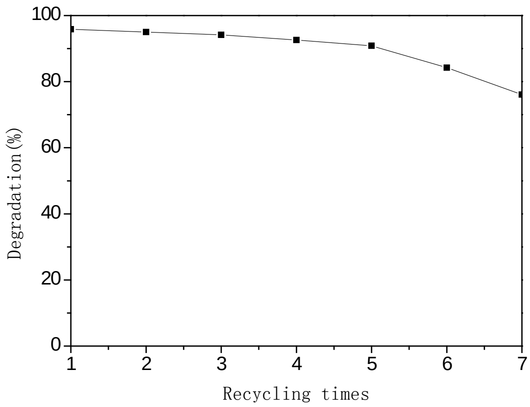

Figure 5. The degradation to MO of sea urchin-like Cu_2O photo-catalyst at different reuse times.

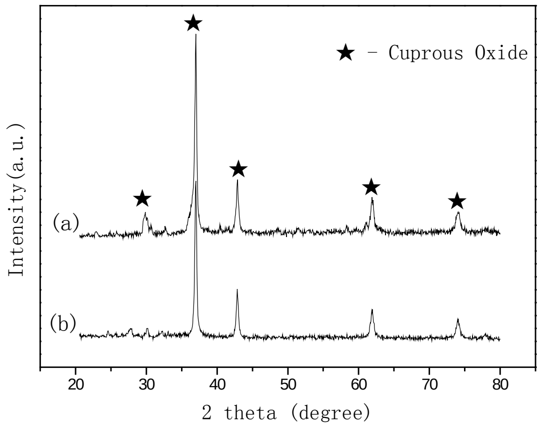

Figure 6. XRD patterns of sea urchin like (a) before use (b) after reuse for seven times.

efficiency and stability.

References

[1] Golob, V., Vinder, A. and Simonic, M. (2005) Effciency of the Coagulation/Flocculation Method for the Treatment of Dye Bath Effluents. *Dyes and Pigments*, **67**, 93-97. http://dx.doi.org/10.1016/j.dyepig.2004.11.003

[2] Yi, F.Y., Chen, S.X. and Yuan, C.E. (2008) Effect of Activated Carbon Fiber Anode Structure and Electrolysis Conditions on Electrochemical Degradation. *Journal of Hazardous Materials*, **157**, 79-87. http://dx.doi.org/10.1016/j.jhazmat.2007.12.093

[3] Garg, V.K., Amita, M. and Kumar, R. (2004) Basic Dye Removal from Simulated Wastewater by Adsorption Using Indian Rosewood Sawdust. *Dyes and Pigments*, **63**, 243-250. http://dx.doi.org/10.1016/j.dyepig.2004.03.005

[4] Molga, E. and Cherbanski, R. (2006) Modeling of an Industrial Full-Scale Plant for Biological Treatment of Textile Wastewaters: Application of Neural Networks. *Industrial & Engineering Chemistry Research*, **45**, 1039-1046. http://dx.doi.org/10.1021/ie050699n

[5] Han, K. and Tao, M. (2009) Electrochemically Deposited p-n Homojunction Cuprous Oxide Solar Cells. *Solid Energy Material Solid Cells*, **93**, 153-158. http://dx.doi.org/10.1016/j.solmat.2008.09.023

[6] Bhosale, M.A., Bhatte, K.D. and Bhanage, B.M. (2013) A Rapid, One Pot Microwave Assisted Synthesis of Nanosize Cuprous Oxide. *Powder Technology*, **235**, 515-519. http://dx.doi.org/10.1016/j.powtec.2012.11.006

[7] Duan, X.J., Gao, R.J. and Zhang, Y.D. (2011) Synthesis of Sea Urchin-Like Cuprous Oxide with Hollow Glass Microspheres as Cores and Its Preliminary Application. *Materials Letters*, **65**, 243-250. http://dx.doi.org/10.1016/j.matlet.2011.07.104

[8] Sui, Y.M., Zen, Y. and Fu, L.L. (2013) Low-Temperature Synthesis of Porous hollow Structured Cu_2O for Photocatalytic Activity and Application. *Royal Society Chemistry Advances*, **40**, 18651-18660.

[9] Duan, X.J., Zhang, Y.D. and Gao, R.J. (2012) Synthesis of 1-D Cuprous Oxide by Using CTAB as a Soft Template in an Acidic System. *Materials Letters*, **68**, 146-148. http://dx.doi.org/10.1016/j.matlet.2011.10.069

[10] Shin, H.S., Song, J.Y. and Yu, J. (2009) Template-Assisted Electrochemical Synthesis of Cuprous Oxide Nanowires. *Materials Letters*, **63**, 397-399. http://dx.doi.org/10.1016/j.matlet.2008.10.052

[11] Jimenez-Cadena, G., Comini, E., Ferroni, M. and Sberveglieri, G. (2010) Synthesis of Cu_2O Bi-Pyramids by Reduction of $Cu(OH)_2$ in Solution. *Materials Letters*, **64**, 469-472. http://dx.doi.org/10.1016/j.matlet.2009.11.051

[12] Liang, Z.H. and Zhu, Y.J. (2005) Synthesis of Uniformly Sized Cu_2O Crystals with Star-Like and Flower-Like Morphologies. *Materials Letters*, **59**, 2423-2425. http://dx.doi.org/10.1016/j.matlet.2005.02.086

[13] Yang, H. and Liu, Z.H. (2010) Facile Synthesis, Shape Evolution, and Photocatalytic Activity of Truncated Cuprous Oxide Octahedron Microcrystals with Hollows. *Crystal Growth & Design*, **10**, 2064-2067.

[14] Tang, A.D., Xiao, Y., Ouyang, J. and Nie, S. (2008) Preparation, Photo-Catalytic Activity of Cuprous Oxide Nano-Crystallites with Different Sizes. *Journal of Alloys and Compound*, **457**, 447-451. http://dx.doi.org/10.1016/j.jallcom.2007.02.148

[15] Huang, L., Peng, F., Yu, H. and Wang, H.J. (2009) Preparation of Cuprous Oxides with Different Sizes and Their

Behaviors of Adsorption, Visible-Light Driven Photocatalysis. *Solid State Sciences*, **11**, 129-138. http://dx.doi.org/10.1016/j.solidstatesciences.2008.04.013

[16] Zhang, X.X., Song, J.M., Jiao, J. and Me, X.F. (2010) Preparation and Photocatalytic Activity of Cuprous Oxides. *Solid State Sciences*, **12**, 1215-1219. http://dx.doi.org/10.1016/j.solidstatesciences.2010.03.009

[17] Sun, W., Sun, W.D. and Zhuo, Y.J. (2011) Facile Synthesis of Cu_2O Nanocube/Polycarbazole Compositesand Their High Visible-Light Photocatalytic Properties. *Journal of Hazardous Material*, **184**, 1628-1643. http://dx.doi.org/10.1016/j.jssc.2011.03.055

[18] Yang, H. and Liu, Z.H. (2010) Facile Synthesis, Shape Evolution, and Photocatalytic Activity of Truncated Cuprous Oxide Octahedron Microcrystals with Hollows. *CrystalGrowth& Design*, **10**, 2064-2067.

[19] Leghari Sajjad, A.K., Shamaila, S. and Tian, B.Z. (2010) Comparative Studies of Operational Parameters of Degradation of Azo Dyes Invisible Light. *Journal of Hazardous Material*, **177**, 781-786.

[20] Tang, D.P., Yuan, R. and Chai, Y.Q. (2006) Ligand-functionalized core/shell Ag@Au nanoparticles labelfree amperometric immunbiosensor. *Biotechnology and Bioengineering*, **94**, 996-1004. http://dx.doi.org/10.1002/bit.20922

[21] Kim, J.Y., Rodriguez, J.A. and Hanson, J.C. (2003) Reduction of CuO and Cu_2O with H_2:H Embedding and Kinetic Effectsinthe Formation of Suboxides. *The Journal American Chemical Society*, **125**, 10684-10692. http://dx.doi.org/10.1021/ja0301673